

ACKNOWLEDGMENTS

The author wishes to thank Dr. D. J. Mickish and Dr. T. L. Gilbert for helpful discussions. He

thanks the staff of the MRL Sigma 5 computer for their aid. Finally he wishes to express his appreciation to Professor R. J. Maurer for his support of this project.

*Work supported in part by the National Science Foundation under Grant No. GH-33634.

¹N. O. Lipari and W. B. Fowler, *Phys. Rev. B* **2**, 3354 (1970); N. O. Lipari, *Phys. Status Solidi* **40**, 691 (1970); N. O. Lipari, *Phys. Rev. B* **6**, 4071 (1972).

²L. Dagens and F. Perrot, *Phys. Rev. B* **5**, 641 (1972).

³A. B. Kunz and D. J. Mickish, *Phys. Rev. B* (to be published).

⁴D. J. Mickish and A. B. Kunz, *J. Phys. C* (to be published).

⁵A. B. Kunz, *J. Phys. C* **3**, 1542 (1970); *Phys. Rev. B* **2**, 5015 (1970); N. O. Lipari and A. B. Kunz, *Phys. Rev. B* **3**, 491 (1971); A. B. Kunz and N. O. Lipari, *J. Phys. Chem. Solids* **32**, 1141 (1971); *Phys. Rev. B* **4**, 1374 (1971); N. O. Lipari and A. B. Kunz, *Phys. Rev. B* **4**, 4649 (1971).

⁶F. Perrot, *Phys. Status Solidi* **52**, 163 (1972).

⁷A. B. Kunz and D. J. Mickish, *J. Phys. C* **6**, L83 (1973).

⁸R. N. Euwema, D. L. Wilhite, and G. T. Surratt, *Phys. Rev. B* **7**, 818 (1973).

⁹F. E. Harris and H. J. Monkhorst, *Phys. Rev. Lett.* **23**, 1026 (1969); *Phys. Rev. B* **7**, 2850 (1973).

¹⁰T. L. Gilbert, in *Molecular Orbitals in Chemistry, Physics, and Biology*, edited by P. O. Löwdin and B. Pullman (Academic, New York, 1964).

¹¹W. H. Adams, *J. Chem. Phys.* **34**, 89 (1961); *J. Chem. Phys.*

37, 2009 (1962).

¹²W. H. Adams, *Chem. Phys. Lett.* **11**, 71 (1971); *Chem. Phys. Lett.* **11**, 441 (1971); *Chem. Phys. Lett.* **12**, 295 (1971).

¹³A. B. Kunz, *Phys. Status Solidi* **36**, 301 (1969).

¹⁴P. W. Anderson, *Phys. Rev. Lett.* **21**, 13 (1968); *Phys. Rev.* **181**, 25 (1969); J. D. Weeks, P. W. Anderson, and A. G. H. Davidson (unpublished).

¹⁵A. B. Kunz, *Phys. Status Solidi* **46**, 697 (1971).

¹⁶J. L. Whitten, *J. Chem. Phys.* **44**, 359 (1966).

¹⁷R. C. McWeeney, in Ref. 10, and references contained therein.

¹⁸P. O. Löwdin, in *Computational Solid State Physics*, edited by F. Herman, N. W. Dalton, and T. R. Koehler (Plenum, New York, 1972), and references contained therein.

¹⁹A. B. Kunz, *Phys. Rev. B* **6**, 606 (1972).

²⁰C. E. Moore, *Atomic Energy Levels*, Nat. Bur. Std. Circ. No. 467 (U.S. GPO, Washington, D. C., 1949), Vol. 1.

²¹*Handbook of Chemistry and Physics*, 48th ed., edited by R. C. Weast and S. M. Selby (Chemical Rubber Co., Cleveland, Ohio, 1967).

²²T. L. Gilbert, in *Sigma Molecular Orbitals Theory*, edited by O. Sinanoğlu and B. Weiburg (Yale U. P., New Haven, Conn., 1969).

Vibration-Induced Absorption (*B* Band) of s^2 -Configuration Ions in Alkali-Halide Crystals*

Taiju Tsuboi[†] and Yoshio Nakai

Department of Physics, Kyoto University, Kyoto, Japan

Keiko Oyama and P. W. M. Jacobs

Department of Chemistry, University of Western Ontario, London, Canada N6A 3K7

(Received 26 February 1973)

A systematic investigation of the optical properties of several ions with the s^2 configuration (In^+ , Sn^{2+} , Tl^+) dissolved in KCl, KBr, and KI has shown that the *B* band, which is the weakest of the three bands that are clearly separated from the fundamental absorption edge, generally has observable structure, particularly at low temperatures. Whereas no structure could be detected for KBr: Tl^+ , a doublet structure was observed for KCl: In^+ , KBr: In^+ , and KCl: Sn^{2+} , and a triplet structure for KBr: Sn^{2+} and KI: Sn^{2+} . As the temperature is raised the *B* band shifts to longer wavelengths in KBr: Sn^{2+} , KI: Sn^{2+} , and KBr: Tl^+ , while it shifts to shorter wavelengths in KBr: In^+ and KCl: In^+ , the magnitude of these shifts being proportional to T . In all the crystals examined the *B*-band intensity increases with temperature as expected for vibration-induced transition. The theoretical line shape for the *B* band is discussed on the basis of various models, and it is concluded that the transition responsible is $^1A_{1g} \rightarrow ^3T_{2u}$ assisted principally by modes of T_{2g} symmetry, but that A_{1g} and E_g modes also play a part. It is also concluded that mixing of the $|A\rangle$ and $|C\rangle$ states with $^3T_{2u}$ is the cause of the observed asymmetry in the *B* band. The position of the *B* band with respect to the *A* and *C* bands is related to the dipole strengths of these bands and the shift of the *B*-band maximum with temperature is due to the quadratic term in the Hamiltonian which is the second-order perturbation from the *A* and *C* states.

I. INTRODUCTION

Alkali-halide crystals containing metal ions with the s^2 configuration exhibit four absorption bands named *A*, *B*, *C*, and *D* on the long-wavelength side

of the fundamental absorption. The assignments for these bands, particularly the *A*, *B*, and *C* bands, have been established as being due to the $s^2 \rightarrow sp$ transition in the metal ion.¹ In particular, the *A* and *C* bands have been assigned to the spin-

orbit allowed ${}^1A_{1g} \rightarrow {}^3T_{1u}$ and dipole allowed ${}^1A_{1g} \rightarrow {}^1T_{1u}$ transitions in the metal ion, respectively. The temperature-sensitive fine structure observed in these bands is caused by the dynamical Jahn-Teller effect in the triply degenerate T_{1u} state.² Because it is the weakest of the four bands, the *B* band has been attributed to the ${}^1A_{1g} \rightarrow {}^3T_{2u}$ and ${}^1A_{1g} \rightarrow {}^3E_u$ transitions, which are forbidden in cubic symmetry. The absorption increases as the temperature is raised, showing that the *B* band is induced by the lattice vibrations. In fact, the temperature dependence of the intensity of the *B* band obeys the theoretical formula for a vibration-induced transition,

$$f(T) = f(0) \coth(\hbar\omega/2kT), \quad (1)$$

where $f(0)$ is the intensity at 0 K, and $\hbar\omega$, k , and T denote the phonon energy, Boltzmann constant, and the thermodynamic temperature, respectively.^{3,4}

Although many papers have been published on the properties of alkali-halide phosphors, these have dealt mainly with the *A* and *C* bands, and there have been few systematic investigations of the *B* band. In the present paper, we report on the optical properties of the *B* band for various ions (In^+ , Sn^{2+} , Tl^+) with the s^2 -configuration ion dissolved in alkali-halide crystals with particular emphasis on the structure of the *B* band and the temperature

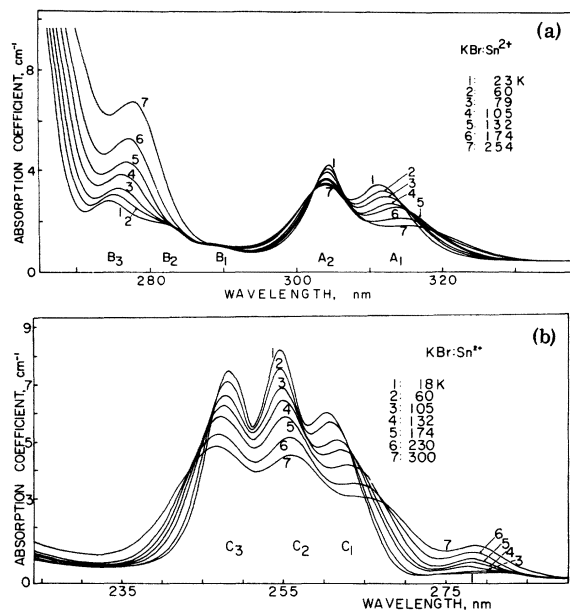


FIG. 1. Temperature dependence of the absorption spectrum of $\text{KBr}:\text{Sn}^{2+}$. Structure in the *A*, *B*, and *C* bands is apparent, particularly at low temperatures. (a) *A* and *B* bands [upper segment of a crystal grown from the melt containing 0.006-mole% SnBr_2]; (b) *B* and *C* bands [lower segment of the same crystal used in (a)].

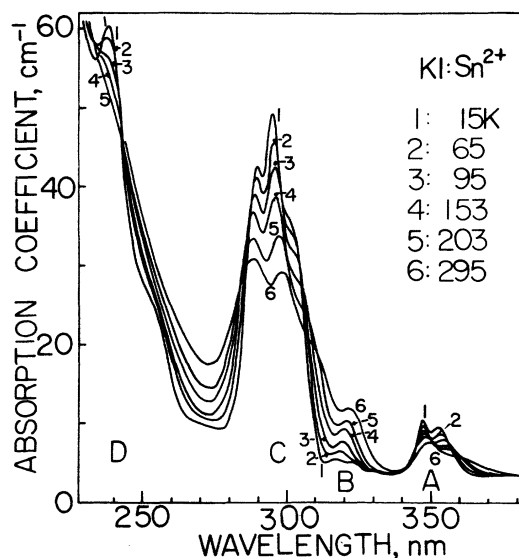


FIG. 2. Temperature-dependence of the absorption spectrum of $\text{KI}:\text{Sn}^{2+}$.

dependence of its peak position and intensity. We shall also discuss correlations between the *B* band and the *A* or *C* band and compare the observed structure of the *B* band with the calculated line-shape function.

II. EXPERIMENTAL PROCEDURE AND RESULTS

Single crystals of $\text{KBr}:\text{In}^+$, Sn^{2+} , or Tl^+ , $\text{KCl}:\text{In}^+$ or Sn^{2+} , and $\text{KI}:\text{Sn}^{2+}$ were grown by the Stockbarger method from KBr powder containing In metal (at a concentration of 0.04 mole%), SnBr_2 powder (0.01 mole%⁵ and 0.006 mole%) or TlBr powder (0.01 mole%), KCl powder containing InCl powder (0.01 mole%⁵) or SnCl_2 powder (0.01 mole%⁵), and KI powder containing SnI_2 powder (0.01 mole%⁵), respectively. The $\text{KBr}:\text{In}^+$ crystal was grown in an atmosphere of 50-torr HBr + 150-torr N_2 , while the other crystals were grown in vacuum. Absorption spectra of the $\text{KBr}:\text{In}^+$, $\text{KBr}:\text{Sn}^{2+}$ (0.006 mole%), $\text{KBr}:\text{Tl}^+$ and $\text{KCl}:\text{Sn}^{2+}$ crystals were measured from liquid-helium temperature to room temperature using a Cary 14R spectrophotometer, while those of the $\text{KBr}:\text{Sn}^{2+}$ (0.01 mole%), $\text{KCl}:\text{In}^+$, and $\text{KI}:\text{Sn}^{2+}$ crystals were measured in the same temperature range using a Shimadzu MPS-50 spectrophotometer at Kyoto University. The CDC 6400 computer at the University of Western Ontario was used to analyze the absorption spectra.

Figures 1–3 show the variation with temperature of the absorption spectra of $\text{KBr}:\text{Sn}^{2+}$, $\text{KI}:\text{Sn}^{2+}$, and $\text{KCl}:\text{Sn}^{2+}$ crystals, respectively. The *A* and *C* bands of these crystals are observed to have temperature-sensitive doublet (A_1 , A_2) and triplet (C_1 , C_2 , C_3) structures, respectively, in agree-

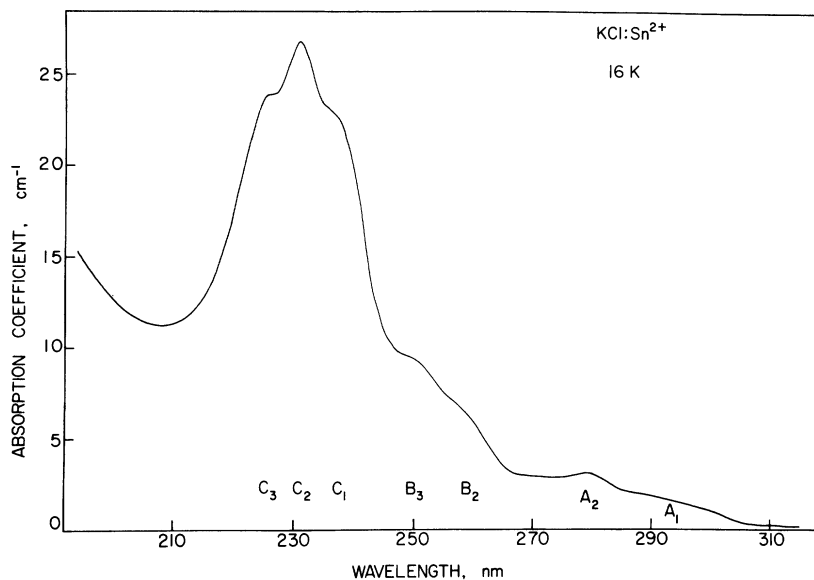


FIG. 3. Absorption spectrum of $\text{KCl}:\text{Sn}^{2+}$ measured at 16 K. The structure in the A, B, and C bands is clearly marked.

ment with the work of Fukuda.^{6,7} We also observed structure in the B band at low temperatures. To illustrate this more clearly, absorption spectra of the B band in $\text{KBr}:\text{Sn}^{2+}$ and $\text{KI}:\text{Sn}^{2+}$ crystals are shown in Figs. 1(a) and 4. The B band of both crystals is composed of three bands (named B_1 , B_2 , and B_3 in order of increasing energy). The same absorption spectra of the B band were obtained in $\text{KBr}:\text{Sn}^{2+}$ crystals grown at Kyoto University and at the University of Western Ontario. In Fig. 5 the absorption coefficients of the B_1 and B_2 peaks are plotted against that of the B_3 peak in KBr crystals containing various concentrations of Sn^{2+} ions. This figure shows that the three components, B_1 , B_2 , B_3 , are due to the same center. The B band in the spectrum of a $\text{KCl}:\text{Sn}^{2+}$ crystal is composed of two bands, which correspond to the B_2 and B_3 bands in $\text{KBr}:\text{Sn}^{2+}$ and $\text{KI}:\text{Sn}^{2+}$. It seems that the other component B_1 was not observed in $\text{KCl}:\text{Sn}^{2+}$ because of the proximity of the A band.

Figures 6 and 7 show the variation with temperature of absorption spectra of $\text{KBr}:\text{In}^+$ and $\text{KCl}:\text{In}^+$ crystals in the region of the B band. The doublet structure of the B band (named B_2 , B_3) is observed at low temperatures in both crystals. The additional bands appearing at 266 nm in $\text{KBr}:\text{In}^+$ and at 248 nm in $\text{KCl}:\text{In}^+$ are attributed to the absorption due to paired In^+ ions.^{6,8} From the intensity ratios of the 248-nm band in KCl crystals containing various concentrations of In^+ ions, and that of the B_3 band, to the B_2 band, the B_2 band is shown not to be due to paired In^+ ions but to be a component of the B band (cf. Ref. 8). The energy separations between the A_1 and A_2 peaks and between the B_2 and

B_3 peaks, which were resolved using the computer, are plotted against $T^{1/2}$ in Fig. 8. The B_2 - B_3 separation, like the A_1 - A_2 separation, is proportional to $T^{1/2}$ at high temperatures and seems to approach a limiting value at low temperatures. Figure 9 shows the temperature variation of the absorption spectrum of a $\text{KBr}:\text{Tl}^+$ crystal in the region of the B band. In this crystal, the B band is observed as a symmetric Gaussian-shaped band with no fine structure.

In Table I, we summarize the observed peak positions of the A, B, and C bands at 20 K and the energy separation between the components of each band in $\text{KBr}:\text{Sn}^{2+}$, $\text{KI}:\text{Sn}^{2+}$, $\text{KBr}:\text{In}^+$, and $\text{KCl}:\text{In}^+$ crystals. As the temperature is raised, the B band is observed to shift to longer wavelengths in $\text{KBr}:\text{Sn}^{2+}$, $\text{KI}:\text{Sn}^{2+}$, and $\text{KBr}:\text{Tl}^+$, while it is observed to shift to shorter wavelengths in $\text{KBr}:\text{In}^+$ and $\text{KCl}:\text{In}^+$. The magnitude of these shifts is proportional to temperature as shown in Fig. 10.

In Fig. 11 the intensities of the B and other bands are plotted against temperature for $\text{KBr}:\text{In}^+$. As the temperature is raised, the intensity of the B band increases in both crystals while that of the A and C bands decrease. The total intensities of the A and B bands is, however, almost independent of temperature in $\text{KBr}:\text{In}^+$. This behavior is similar to those observed in $\text{KCl}:\text{In}^+$ by Fukuda⁷ and in $\text{KCl}:\text{Ag}^-$ by Kleemann.⁹

III. LINE-SHAPE FUNCTION FOR B BAND

In this section we shall calculate the line-shape function for the B band. The s^2 -configuration ion has the ground-state $^1A_{1g}$ in cubic symmetry. The lowest excited states arise from the sp configura-

tion and are the ${}^3T_{1u}$, ${}^3T_{2u}$, 3E_u , and ${}^1T_{1u}$ states. The ${}^3T_{1u}$ and ${}^1T_{1u}$ states are mixed by spin-orbit interaction leading to the excited states of the A and C bands

$$|A\rangle = -\nu |{}^1T_{1u}\rangle + \mu |{}^3T_{1u}\rangle, \quad (2)$$

$$|C\rangle = \mu |{}^1T_{1u}\rangle + \nu |{}^3T_{1u}\rangle, \quad (3)$$

where μ and ν are the mixing coefficients. The B state (the excited state of the B band) is

$$|B\rangle = |{}^3T_{2u}\rangle \text{ and } |{}^3E_u\rangle. \quad (4)$$

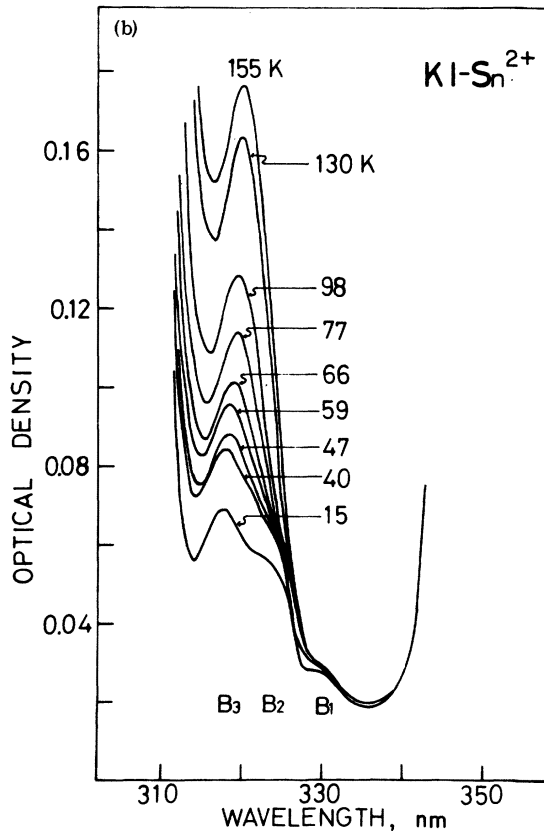
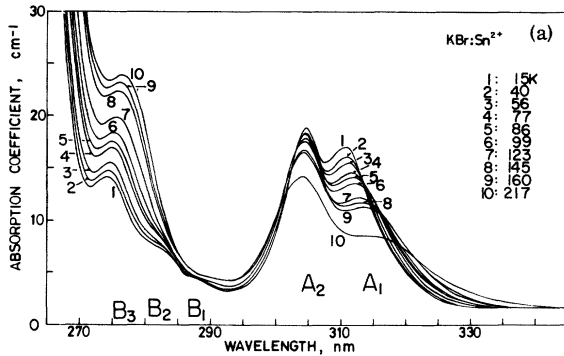


FIG. 4. Structure in the B band shown by absorption spectra of (a) KBr:Sn²⁺ (0.01 mole%) (Ref. 5), and (b) KI:Sn²⁺ (0.01 mole%) (Ref. 5) at various temperatures.

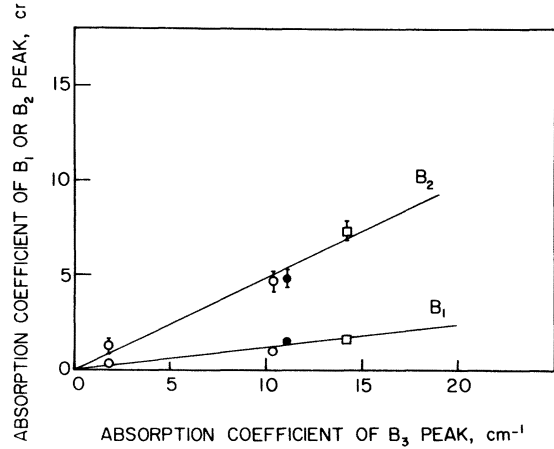


FIG. 5. Linear relations between the absorption coefficient at the peak of the B₁ or B₂ bands and that of the B₃ band for KBr:Sn²⁺, containing various concentrations of Sn²⁺ ions, at 20 K. The filled symbols denote a crystal grown and measured at Kyoto University. The squares denote a quenched crystal.

These states have linear interactions with the lattice vibrations of the A_{1g} mode (interaction mode coordinate Q₁ according to Toyozawa and Inoue²), E_g mode (Q₂, Q₃), and T_{2g} mode (Q₄, Q₅, Q₆). The matrix of the electron-lattice interaction can be written¹⁰

$$\underline{M} + aQ_1 \underline{1}, \quad (5)$$

where the components of \underline{M} are given in Table II. a , b , and c are the coupling constants and b_1 , b_2 , c_1 , and c_2 are defined by

$$b_1 = (\mu^2 - \frac{1}{2}\nu^2)b, \quad b_2 = (\nu^2 - \frac{1}{2}\mu^2)b, \quad (6)$$

$$c_1 = (\mu^2 - \frac{1}{2}\nu^2)c, \quad c_2 = (\nu^2 - \frac{1}{2}\mu^2)c.$$

In the semiclassical Franck-Condon approximation, the line-shape function for the transition ${}^1A_{1g} \rightarrow B$ is given by¹¹

$$F(E) = \int dQ |P_B(Q)|^2 e^{-U_0(Q)/kT} \times \delta(U_B(Q) - U_0(Q) - E) / \int dQ e^{-U_0(Q)/kT}, \quad (7)$$

where $P_B(Q)$ is the dipole moment matrix element for the transition, E is the energy of incident photon, and $U_B(Q)$, $U_0(Q)$ are the adiabatic potentials of the B state and the ground state as a function of the coordinates, Q . Thus^{2,12}

$$U_0(Q) = \sum_{i=1}^6 Q_i^2.$$

To simplify the calculation, we assume that the force constants are the same in both the states. The symmetry of the B band in KBr:Ti³⁺ shows this to be a reasonable approximation. The effective temperature is¹³

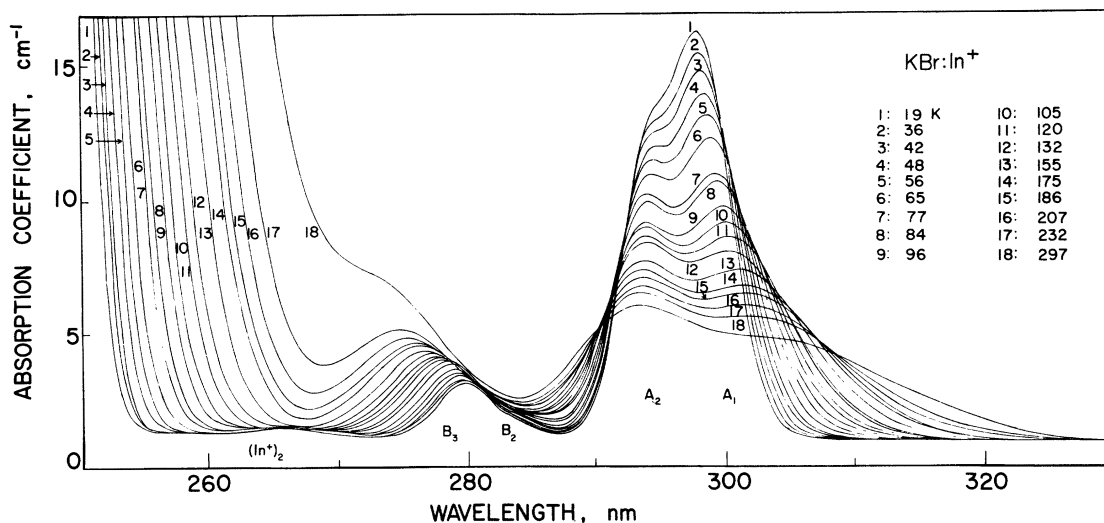


FIG. 6. Temperature dependence of the absorption spectrum of KBr:In⁺. A doublet structure B₂, B₃ is observed in the B band. The band at 266 nm is due to (In³⁺)₂.

$$T^* = (\epsilon/2k) \coth(\epsilon/2kT).$$

The forbidden transitions $^1A_{1g} \rightarrow ^3T_{2u}$ and 3E_u are made allowed by the mixing of the B state with the A and C states. If the $^1A_{1g} \rightarrow ^3T_{2u}$ transition is the only contribution to the B band, the effective $|P_B(Q)|^2$ can be written¹⁴

$$|P_{^3T_{2u}}(Q)|^2 = \mu^2 \nu^2 |\langle \alpha | \hat{P}_\eta | z \rangle|^2 \left(\frac{1}{E_{BA}} + \frac{1}{E_{CB}} \right)^2 \times \left[\frac{3}{2} b^2 (Q_2^2 + Q_3^2) + \frac{1}{2} c^2 (Q_4^2 + Q_5^2 + Q_6^2) \right], \quad (8)$$

where \hat{P}_η is the dipole moment operator, and α and z stand for the eigenfunctions of the s and p states, respectively. $E_{BA} (= E_B - E_A)$ means the energy separation between the B and A states and $E_{CB} (= E_C - E_B)$ is the separation between the C and B states. Similarly, for the $^1A_{1g} \rightarrow ^3E_u$ tran-

sition,

$$|P_{^3E_u}(Q)|^2 = \mu^2 \nu^2 |\langle \alpha | \hat{P}_\eta | z \rangle|^2 \left(\frac{1}{E_{BA}} + \frac{1}{E_{CB}} \right)^2 \times c^2 (Q_4^2 + Q_5^2 + Q_6^2). \quad (9)$$

In the derivation of the adiabatic potentials $U_{^3T_{2u}}$ and $U_{^3E_u}$, we temporarily neglect the matrix elements connecting the $^3T_{2u}$ or 3E_u state and other states in (5).

First, we calculate the shape function for the $^1A_{1g} \rightarrow ^3E_u$ transition. Making use of (9) and the eigenvalues, which are easily obtained from the two-dimensional matrix for the 3E_u state in (5), we get

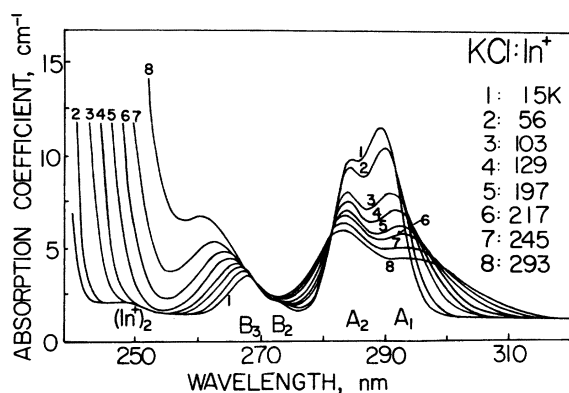


FIG. 7. Temperature-dependence of the absorption spectrum of KCl:In⁺. A doublet structure B₂, B₃ is observed in the B band. The band at 248 nm is due to (In³⁺)₂.

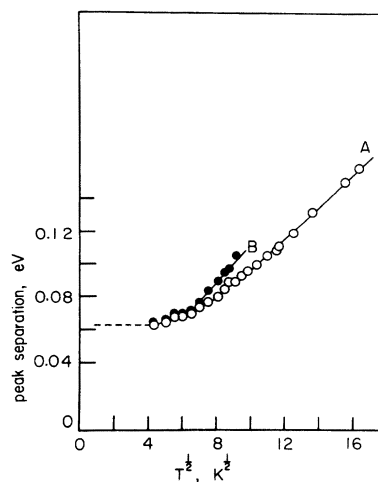


FIG. 8. Peak separation in the A and B bands in KBr:In⁺ in eV as a function of $T^{1/2}$. Curve A is for the difference A_2-A_1 and curve B for the difference B_3-B_2 .

TABLE I. Peak positions and peak separation of the A, B, and C bands at 20 K, in eV.

	A_1	A_2	A_2-A_1	B_1	B_2	B_3	B_2-B_1	B_3-B_2	C_1	C_2	C_3	C_2-C_1	C_3-C_2
KBr:Sn ²⁺ ^a	3.986	4.080	0.094	4.260	4.394	4.508	0.134	0.114	4.763	4.883	5.004	0.120	0.121
KI:Sn ²⁺	3.515	3.573	0.058	3.77	3.85	3.90	0.08	0.05	4.14	4.205	4.280	0.06	0.08
KCl:Sn ²⁺	4.29	4.43	0.14	4.84	4.98			0.14	5.240	5.375	5.500	0.13	0.13
KBr:In ³⁺	4.162	4.225	0.063	4.366	4.429			0.063					
KCl:In ³⁺	4.286	4.357	0.071	4.56	4.632			0.07					

^aBands resolved by computer analysis.

$$F_{3E_u}(E) = \frac{9Kc^2}{4b^2} |E - W_{3E_u}| \exp\left(\frac{-3(E - W_{3E_u})^2}{b^2 kT^*}\right), \quad (10)$$

where W_{3E_u} is the excitation energy at $Q_i = 0$ ($i = 1, 2, 3, 4, 5, 6$) and

$$K = \mu^2 \nu^2 |\langle \alpha | \hat{P}_\eta | z \rangle|^2 \left(\frac{1}{E_{BA}} + \frac{1}{E_{CB}} \right)^2. \quad (11)$$

Equation (10) gives a line shape which is completely split into two bands as shown in Fig. 12. The splitting of the two peaks is proportional to $\coth^{1/2}(\epsilon/2kT)$, and the total intensity of the two bands to $\coth(\epsilon/2kT)$.

Next, we calculate the shape function for the other transition ${}^1A_{1g} \rightarrow {}^3T_{2u}$. When we take into account only the E_g mode in (5), we obtain the following shape function:

$$F_{3T_{2u}}(E; E_g) = \frac{3\sqrt{3}K|b|}{8} \left(\frac{kT^*}{\pi}\right)^{1/2} \left(1 + \frac{2(E - W_{3T_{2u}})^2}{b^2 kT^*}\right) \times \exp\left(\frac{-3(E - W_{3T_{2u}})^2}{b^2 kT^*}\right). \quad (12)$$

Equation (12) gives a single band with a symmetric line shape.

Secondly, we take into account only the T_{2g} mode

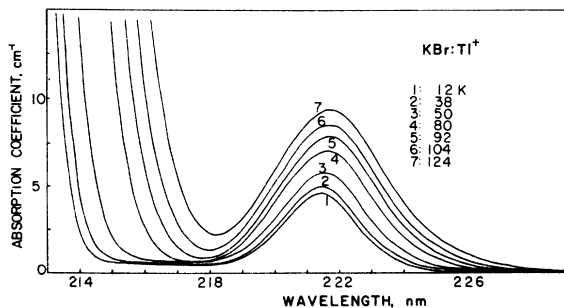


FIG. 9. Temperature dependence of the absorption spectrum of KBr:Ti³⁺ in the region of the B band. No fine structure is observed for the B band in this instance.

in (5). The matrix for the ${}^3T_{2u}$ state is entirely analogous to ones for the A and C states except for the coefficients of the coupling constants. The eigenvalues of the matrix for the C state have been obtained by Toyozawa and Inoue² and by Honma.¹⁰ Making use of their results, we have $\frac{1}{2}cQt_i(\lambda)$

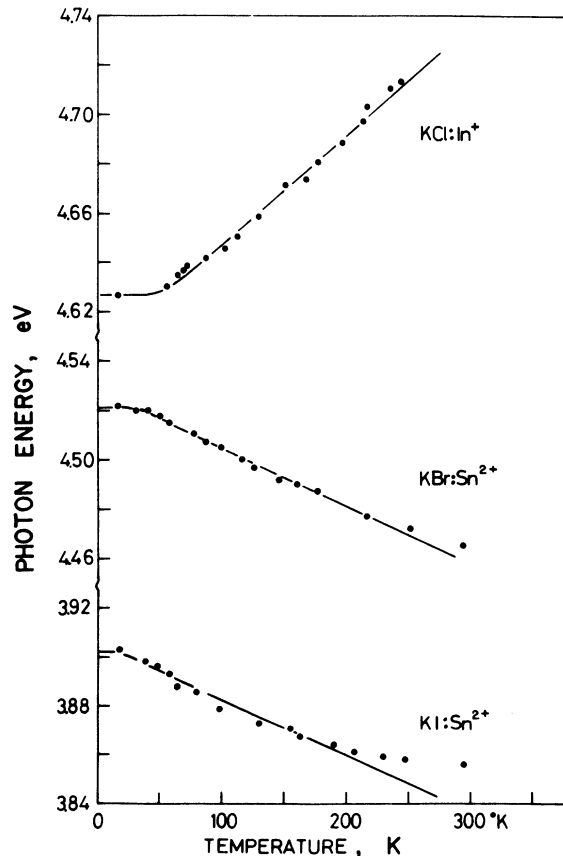


FIG. 10. Temperature-dependence of the position of maximum absorption in the B band for KCl:In³⁺, KBr:Sn²⁺, and KI:Sn²⁺.

TABLE II. Elements of the matrix \bar{M} which describes the electron-lattice interaction for symmetry coordinates $Q_2, Q_3 (E_g)$ and $Q_4, Q_5, Q_6 (T_{2g})$. The A_{1g} mode (coordinate Q_1) adds a term aQ_1 to each diagonal element.

C>		B>			A>			
x	y	z	T _{2u}	E _u	x	y	z	
$b_1 \left(Q_2 - \frac{Q_3}{\sqrt{3}} \right)$	$c_1 Q_6$	$c_1 Q_5$	$\frac{i\nu}{2} c Q_6$	$\frac{i\nu}{2} c Q_4$	$\frac{i\sqrt{3}}{2} \nu c Q_4$	$-\frac{3}{2} \mu \nu b \left(Q_2 - \frac{Q_3}{\sqrt{3}} \right)$	$-\frac{3}{2} \mu \nu c Q_6$	$-\frac{3}{2} \mu \nu c Q_5$
$-b_1 \left(Q_2 + \frac{Q_3}{\sqrt{3}} \right)$	$c_1 Q_4$	$c_1 Q_4$	$-\frac{i\nu}{2} b (Q_2 - \sqrt{3} Q_3)$	$\frac{i\nu}{2} c Q_5$	$-\frac{i\sqrt{3}}{2} \nu c Q_5$	$-\frac{3}{2} \mu \nu b \left(Q_2 + \frac{Q_3}{\sqrt{3}} \right)$	$\frac{3}{2} \mu \nu b \left(Q_2 + \frac{Q_3}{\sqrt{3}} \right)$	$-\frac{3}{2} \mu \nu c Q_4$
	$\frac{2}{\sqrt{3}} b_1 Q_3$	$\frac{i\nu}{2} c Q_5$	$-\frac{i\nu}{2} c Q_4$	$i\nu b Q_2$	0	$-\frac{3}{2} \mu \nu c Q_5$	$-\frac{3}{2} \mu \nu c Q_4$	$-\sqrt{3} \mu \nu b Q_3$
	$-\frac{b}{2} \left(Q_2 - \frac{Q_3}{\sqrt{3}} \right)$	$\frac{c}{2} Q_4$	$\frac{c}{2} Q_4$	$-\frac{c}{2} Q_4$	$\frac{c}{2\sqrt{3}} Q_4$	$\frac{i\mu}{2} b (Q_2 + \sqrt{3} Q_3)$	$\frac{i\mu}{2} c Q_6$	$-\frac{i\mu}{2} c Q_5$
	$\frac{b}{2} \left(Q_2 + \frac{Q_3}{\sqrt{3}} \right)$	$\frac{c}{2} Q_4$	$\frac{c}{2} Q_4$	$\frac{c}{2} Q_5$	$\frac{c}{2\sqrt{3}} Q_5$	$-\frac{i\mu}{2} c Q_6$	$\frac{i\mu}{2} b (Q_2 - \sqrt{3} Q_3)$	$\frac{i\mu}{2} c Q_4$
		$-\frac{b}{\sqrt{3}} Q_3$	$-\frac{b}{\sqrt{3}} Q_3$	0	$-\frac{c}{\sqrt{3}} Q_6$	$\frac{i\mu}{2} c Q_5$	$-\frac{i\mu}{2} c Q_4$	$-i\mu b Q_2$
		$-\frac{b}{\sqrt{3}} Q_3$	$-\frac{b}{\sqrt{3}} Q_3$	$-\frac{b}{\sqrt{3}} Q_3$	$-\frac{b}{\sqrt{3}} Q_2$	$-\frac{i\mu}{2} c Q_4$	$\frac{i\mu}{2} c Q_5$	$i\mu c Q_6$
				$\frac{b}{\sqrt{3}} Q_3$	$-\frac{b}{\sqrt{3}} Q_3$	$-\frac{i\sqrt{3}}{2} \mu c Q_4$	$\frac{i\sqrt{3}}{2} \mu c Q_5$	0
					$b_2 \left(Q_2 - \frac{Q_3}{\sqrt{3}} \right)$	$c_2 Q_6$	$c_2 Q_5$	$c_2 Q_4$
					$-b_2 \left(Q_2 + \frac{Q_3}{\sqrt{3}} \right)$	$-b_2 \left(Q_2 + \frac{Q_3}{\sqrt{3}} \right)$	$c_2 Q_4$	$\frac{2}{\sqrt{3}} b_2 Q_3$

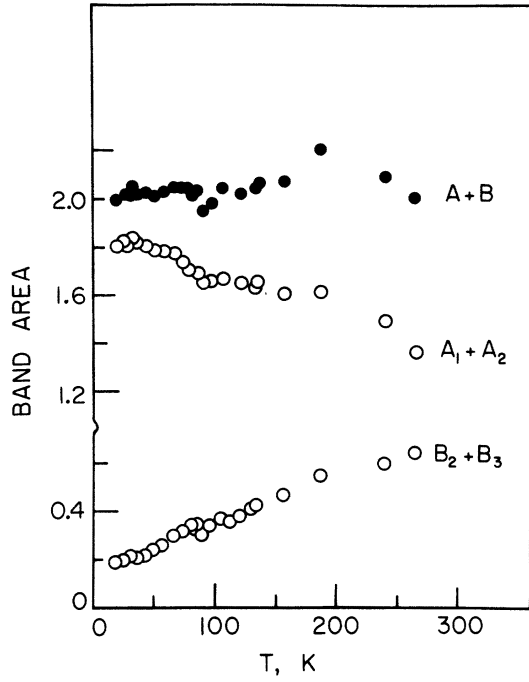


FIG. 11. Intensity of the A and B bands in KBr:In* as functions of temperature. $A_1 + A_2$ means the sum of the band areas for the two components of the A band. Similarly the curve marked $B_2 + B_3$ is the sum of the areas of the two components of the B band below 90 K. Above 90 K the B band was treated as a single band and so $B_2 + B_3$ is the total area of this band. The curve marked A+B is the total area of the A and B bands.

$i = 1, 2, 3$) as the eigenvalues of the ${}^3T_{2u}$ state, where

$$Q = (Q_4^2 + Q_5^2 + Q_6^2)^{1/2},$$

$$t_1(\lambda) = -\frac{2}{\sqrt{3}} \cos \frac{l-\pi}{3}, \quad t_2(\lambda) = \frac{2}{\sqrt{3}} \cos \frac{l+\pi}{3},$$

$$t_3(\lambda) = \frac{2}{\sqrt{3}} \cos \frac{l}{3}, \quad (13)$$

$$\cos l = \frac{2}{3} \sqrt{3} \lambda, \quad \lambda = 2Q_4 Q_5 Q_6 / Q^3.$$

The line-shape function for the ${}^1A_{1g} \rightarrow {}^3T_{2u}$ transition is then

$$F_{3T_{2u}}(E; T_{2g}) = \frac{c^2 K (\pi k T^*)^{-3/2}}{18} \sum_{i=1}^3 \int \frac{d\Omega}{d\lambda} d\lambda dQ Q^4 e^{-Q^2/k T^*} \\ \times \delta(E - W_{3T_{2u}} - cQ t_i(\lambda)/2). \quad (14)$$

In this calculation we have used the following approximation for each component of the dipole strength:

$$|P_{3T_{2u}}(Q)|^2 = Kc^2 \langle \alpha | \hat{P}_\eta | z \rangle \left| \frac{1}{6} (Q_4^2 + Q_5^2 + Q_6^2) \right|.$$

To simplify the analysis we change the independent variable and denote the line-shape function by $f(x)$, defined by

$$F(E) dE = f(x) dx, \quad x = 2(E - W_{3T_{2u}}) / (c^2 k T^*)^{1/2}. \quad (15)$$

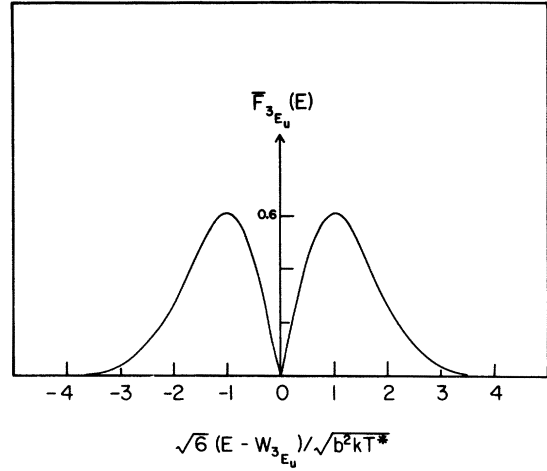


FIG. 12. Normalized line-shape function $\bar{F}_{3E_u} = F_{3E_u}(E) / (9Kc^2/4b^2)$ [Eq. (10)] for the transition ${}^1A_{1g} \rightarrow {}^3E_u$ assuming that the 3E_u state interacts only with the $E_g(Q_2, Q_3)$ modes. E is the photon energy and the predicted line shape on this model is a band completely split into two symmetrical parts about $E = W_{3E_u}$.

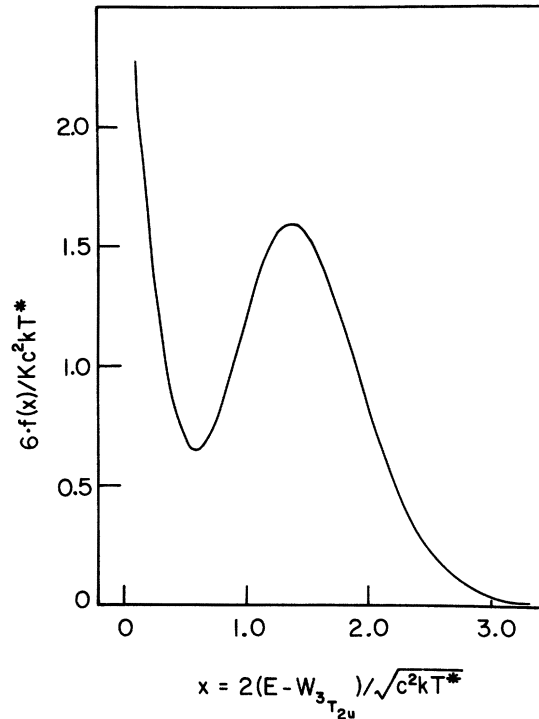


FIG. 13. Line-shape function $f(x)/Kc^2 k T^*$ given by Eq. (16) for the model which assumes that the B state is derived from ${}^3T_{2u}$ and interacts only with the $T_{2g}(Q_4, Q_5, Q_6)$ modes. The band shape is symmetrical about $E = W_{3T_{2u}}$. This model predicts a triplet structure for the B band with a logarithmic singularity at $E = {}^3T_{2u}$ due to the fact that $t_2(\lambda) \rightarrow 0$ as $\lambda \rightarrow 0$. This singularity will be smoothed out by additional interactions with the A_{1g} and E_g modes.

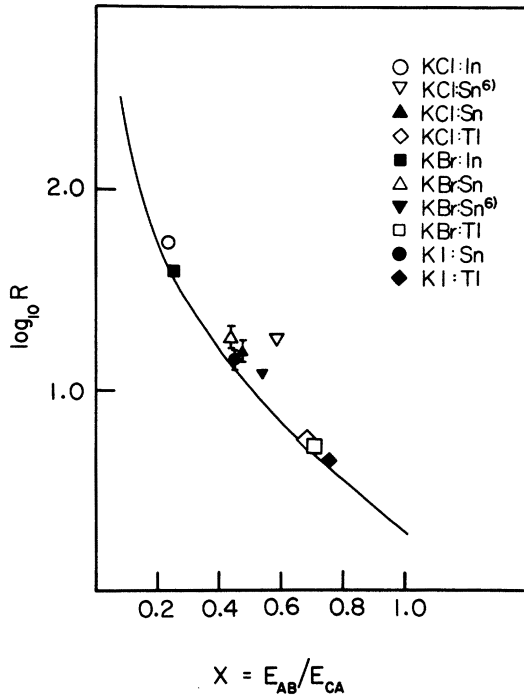


FIG. 14. Plot of $\log_{10} R$, where R is the ratio of the dipole strengths of the C and A bands, against E_{BA}/E_{CA} . The continuous line has been calculated from Sugano's formula, Eq. (19), and the various symbols indicate experimental data.

We can then write $f(x)$ as

$$f(x) = \frac{Kc^2 k T^* \pi^{-3/2}}{18} \sum_{i=1}^3 \int \frac{x^4}{|t_i^5(\lambda)|} e^{-x^2/t_i^2(\lambda)} \frac{d\Omega}{d\lambda} d\lambda. \quad (16)$$

We have evaluated the line-shape function (16) numerically and the result of this calculation is shown in Fig. 13. It should be noted that the line shape of Fig. 13 is similar to the shape of the C band as calculated by Toyozawa and Inoue.² The splitting on either side in Fig. 13 is $0.68 (c^2 k T^*)^{1/2}$, while that in the C band² is $0.91 (c^2 k T^*)^{1/2}$. If the shape function, Eq. (16), is integrated over x , the total intensity is proportional to T^* . The logarithmic singularity at $E = W_{3T_{2u}}$ is removed if the interactions with A_{1g} and E_g modes are taken into account: A triplet-structure is then obtained for the B band.

IV. DISCUSSION

A. Fine Structure of the B Band

As mentioned in Sec. II, the B band in $KBr : Sn^{2+}$ and $KI : Sn^{2+}$ has a triplet structure at low temperatures. Of the three possible models considered in Sec. III, only the shape function (14) explains the triplet structure. This implies that the B band is caused mainly by the $^1A_{1g} - ^3T_{2u}$ transition, which is in agreement with the results of the effect of

uniaxial stress on the B band absorption by Bimberg *et al.*¹⁵

So far, we have neglected the mixing of the $^3T_{2u}$ state with the other states in the calculation of the eigenvalues of the $^3T_{2u}$ state. Making use of (5), the effective interaction Hamiltonian for the $^3T_{2u}$ state coupled with the T_{2g} mode can be written approximately as

$$H_{e1}(^3T_{2u}; T_{2g}) = \frac{1}{2} c \underline{T} Q + c^2 \left(\frac{\mu^2}{E_{BA}} - \frac{\nu^2}{E_{CB}} \right) \left(\underline{1} - \frac{1}{2} \underline{T}^2 \right) Q^2, \quad (17)$$

where $\underline{1}$ is the three-dimensional unit matrix, and

$$\underline{T} = Q^{-1} \begin{pmatrix} 0 & Q_6 & Q_5 \\ Q_6 & 0 & Q_4 \\ Q_5 & Q_4 & 0 \end{pmatrix}. \quad (18)$$

The quadratic term of (17), which is due to the $A - ^3T_{2u}$ mixing and the $C - ^3T_{2u}$ mixing, would explain the asymmetry of the B band seen in Fig. 4. This is because (17) is analogous to the interaction Hamiltonian for the C state given by Toyozawa and Inoue,² and the asymmetry of the triplet-structured C band has been explained by the quadratic term in the Hamiltonian.¹⁶

Next, we discuss the doublet structure of the B band observed in $KBr : In^+$ and $KCl : In^+$. The coefficient $c^2(\mu^2/E_{BA} - \nu^2/E_{CB})$ of the quadratic term in (17) has almost the same value in both $KCl : In^+$ and $KI : Sn^{2+}$; this was estimated using the values of c^2 given by Toyozawa and Inoue.² The same is true for the coefficient $\frac{1}{2}c$ of the linear term in (17). Therefore, we expect theoretically that the B band of $KCl : In^+$ should have a triplet structure like that of $KI : Sn^{2+}$ and the separation between the components be proportional to $T^{*1/2}$ (see Sec. III). In fact, the $B_2 - B_3$ separation in $KBr : In^+$ increases in proportion to $T^{1/2}$ at high temperatures, as shown in Fig. 8. We suggest therefore that another component of the B band in $KCl : In^+$, which corresponds to the B_1 band in $KI : Sn^{2+}$, lies hidden in the tail of the A_2 band. The same would be true for $KBr : In^+$.

The B band of $KBr : Tl^+$ has little structure, in contrast with the spectra due to Sn^{2+} and In^+ ions. This is due to the fact that the A and C bands have little visible fine structure because of the small value of the coupling constant c .¹⁷

B. Position of B Band in Absorption Spectrum

In 1962 Sugano¹⁸ obtained the following formula (named Sugano's formula) using the molecular-orbital model for the $s^2 - sp$ transition. It relates the positions of the A , B , and C bands to their dipole strengths¹⁰:

$$E_{BA}/E_{CA} = [1 + (2R)^{1/2}] / (R + 1). \quad (19)$$

Here R is the ratio of the dipole strengths of the C

and *A* bands, i. e., $R = \mu^2/\nu^2$. In Fig. 14, we have plotted the ratio R calculated from Sugano's formula and the observed ratio R at 20 K against E_{BA}/E_{CA} . When the *A*, *B*, and *C* bands display fine structure, the centers of the bands were used for the positions, e. g., for the Sn^{2+} ion the energy of the B_2 peak was taken as W_B . The ambiguity in the values of R of $\text{KBr}:\text{Sn}^{2+}$, $\text{KI}:\text{Sn}^{2+}$, and $\text{KCl}:\text{Sn}^{2+}$ shown in Fig. 14 comes from the overlap of the *C* band with the fundamental absorption band. It is seen that the experimental points fit the theoretical Sugano formula quite well. It should be noted that the discrepancies between Sugano's formula and the experimental points, which were observed in the cases of Sn^{2+} and In^+ ions by Fukuda,⁶ are much improved by making use of the exact center of the *B* band for the energy of the *B* band. Thus, we can explain the following experimental facts on the position of the *B* band by Sugano's formula: The position of the *B* band is near the *C* band for those ions (Tl^+) for which the value of R is comparatively small ($R \sim 5$); it is near the *A* band for those ions (In^+) for which R is comparatively large ($R \sim 50$); and it is nearly halfway between the *A* and *C* bands for Sn^{2+} ions for which $R = 15-20$.

We have also observed in Sec. III that the *B* band in alkali halides doped with Sn^{2+} and Tl^+ exhibits a red shift as the temperature is raised, while it exhibits a blue shift in the In^+ -doped salts. This

behavior seems to be due to the quadratic term Q^2 in (17), which is the second-order perturbation from the *A* and *C* states. Owing to this perturbation, the energy of the *B* state in Tl^+ ions is repelled by the closely lying *C* state, while in In^+ ions it is repelled by the closely lying *A* state. In the cases of Sn^{2+} ions, it is repelled by the overlapping *C* state. The thermal average of Q^2 is proportional to $\coth(\epsilon/2kT)$; therefore the *B* band shifts linearly with temperature T , as seen in Fig. 10. We cannot, however, neglect the effect of thermal expansion¹⁹ on the band shift. In some alkali-halide phosphors containing Tl^+ , which have almost the same values of R and E_{BA}/E_{CA} , the *B* band is observed to shift differently as the temperature increases. The red shift of the *B* band of $\text{KI}:\text{Tl}^+$ is larger than that of $\text{KBr}:\text{Tl}^+$, while in $\text{KCl}:\text{Tl}^+$ the shift is hardly appreciable. Also, in $\text{KI}:\text{Tl}^+$ the *A* and *C* bands also exhibit a red shift as the temperature is raised while in $\text{KCl}:\text{Tl}^+$ they exhibit little shift like the *B* band.³

ACKNOWLEDGMENTS

We thank the National Research Council of Canada for their support of that part of this research performed at the University of Western Ontario. We should also like to acknowledge the contribution of Mrs. Sheila A. Thorsley who wrote or adapted many of the computer programs used.

*Publication No. 69 from the Photochemistry Unit, University of Western Ontario.

†On leave of absence from Kyoto Sangyo University, Kyoto, Japan at University of Western Ontario, London, Canada.

¹W. B. Fowler, in *Physics of Color Centers*, edited by W. B. Fowler (Academic, New York, 1968).

²Y. Toyozawa and M. Inoue, *J. Phys. Soc. Jap.* **21**, 1663 (1966).

³T. Tsuboi and R. Kato, *J. Phys. Soc. Jap.* **27**, 1192 (1969).

⁴K. Füssgäenger, *Phys. Status Solidi* **36**, 645 (1969).

⁵These crystals were grown at the Department of Physics, Kyoto University, Japan.

⁶A. Fukuda, *Sci. Light* **13**, 64 (1964).

⁷A. Fukuda, *J. Lumin.* **1/2**, 376 (1970).

⁸T. Tsuboi, *J. Phys. Soc. Jap.* **29**, 1303 (1970).

⁹W. Kleeman, *Z. Phys.* **234**, 362 (1970).

¹⁰A. Honma, *J. Phys. Soc. Jap.* **24**, 1082 (1968).

¹¹S. Sugano, Y. Tanabe, and H. Kamimura, *Multiplets of Transition Metal Ions in Crystals* (Academic, New York, 1970).

¹²K. Cho, *J. Phys. Soc. Jap.* **25**, 1372 (1968).

¹³M. Lax, *J. Chem. Phys.* **20**, 1752 (1952); P. R. Moran, *Phys. Rev.* **137**, A1016 (1965).

¹⁴First-order nondegenerate perturbation theory has been used for the mixing of the *C* and *A* states with the *B* state via the electron-lattice interaction Eq. (5).

¹⁵D. Bimberg, W. Dultz, and K. Füssgäenger, *Phys. Lett. A* **25**, 766 (1967).

¹⁶A. Honma, *Sci. Light* **18**, 33 (1969).

¹⁷In a detailed analysis of the absorption spectra of $\text{KBr}:\text{Tl}^+$, the *A* band has nevertheless been resolved successfully into two components at low temperatures (< 80 K) and into three components at high temperatures (> 80 K) [P. W. M. Jacobs and Sheila A. Thorsley (unpublished)].

¹⁸S. Sugano, *J. Chem. Phys.* **36**, 122 (1962).

¹⁹P. W. M. Jacobs and Lesley M. Parsons, *Cryst. Lattice Defects* **3**, 155 (1972).